# Modelling pressure drop-velocity relationships in large round bales of alfalfa herbage

Y.D. YILJEP[1], W.K. BILANSKI[2] and D.M. JOY[2]

*[1]NAERLS/Ahmadu Bello University, P.M.B. 1067, Zaria, Nigeria; [2]School of Engineering, University of Guelph, Guelph, ON, Canada N1G 2W1.* *Received 15 December 1991; accepted 5 November 1992.*

Yiljep, Y.D., Bilanski, W.K. and Joy, D.M. 1992. **Modelling pressure drop-velocity relationships in large round bales of alfalfa herbage**. Can. Agric. Eng. **34**:383-391. The resistance to airflow through high-moisture soft-centre large round bales of alfalfa herbage was determined for air velocities between 1.0 and 1.5 m/s. A general one-dimensional mathematical model relating pressure gradient and fluid velocity was developed based upon the concept of fluid flow in porous media. The model was further modified by assuming that for a characteristic alfalfa crop harvested in round bales, the length of an alfalfa stem is much greater than its diameter; thus, the aspect ratio is negligible. Global viscous and inertial coefficients were predicted from the general and reduced models across bale axial lengths. Viscous forces dominated in planes around bale axial centres with inertial forces pronounced in planes near inlet and outlet faces. In general, the bales were found to be significantly denser in their axial centres than in the inlet and outlet portions.

La résistance à l'écoulement d'air au travers de grosses balles rondes de luzerne humide a été déterminée pour des vitesses d'air variant entre 1.0 et 1.5 m/s. Un modèle mathématique général et unidimensionnel reliant le gradient de pression et la vitesse d'un fluide a été développé à partir du concept d'écoulement d'un fluide en milieu poreux. Le modèle a par la suite été modifié en supposant que, pour la luzerne récoltée en balles rondes, la longueur des tiges est beaucoup plus large que le diamètre de la plante; ainsi, le rapport d'exposition est négligeable. Les coefficients globaux de viscosité et d'inertie ont été prédits à partir du modèle général et du modèle modifié appliqués sur des longueurs axiales des balles. Les forces de viscosité ont dominé dans les plans situés autour des centres axiaux des balles, et les forces d'inertie ont été prononcées dans les plans situés près des extrémités des axes. En général, les balles ont été trouvées comme étant significativement plus denses dans leurs centres axiaux que dans les portions situées aux extrémités.

## INTRODUCTION

Large round bales have become a familiar sight throughout North America in recent years. The ability to harvest hay with less labour and at a greater rate has held great appeal to hay and livestock producers. Balers harvest and package hay into manageable units for transport, storage, and feeding. Recent statistics (Anon 1989), showing the sales of large round balers in North America to be double those of conventional square balers, give further evidence of their general acceptance.

The successful design of a ventilation system for drying (cooling) and aerating stored agricultural commodities depends upon a knowledge of pressure and airflow distribution in relation to size and shape as well as upon the characteristics of the commodity and of the air. The resistance to airflow of many agricultural products has been extensively reviewed and reported in the literature (Segerlind 1983; Jayas et al. 1987). Flow through low-moisture hard-centre large round bales of hay has been studied (Marchant 1976a; Rotz 1983) but a much smaller amount of information is available for soft-centre high-moisture large round bales of alfalfa herbage. Plue and Bilanski (1991) have studied some general flow characteristics of flow through soft-centre bales. However, their setup was such that information on the pressure gradient-apparent velocity relationships were not able to be determined. The purpose of this study was to develop and verify a one-dimensional mathematical model for predicting pressure gradient-apparent velocity relationships in large round bales of alfalfa herbage for given ambient weather conditions indicated by absolute viscosity and density of air as well as bale particle size characteristics. Porosity variation in the bales will be predicted and reported in another paper.

## FLOW THROUGH POROUS AGRICULTURAL PRODUCTS

A porous medium was defined by Collins (1961) as a solid containing pores or voids of sufficient number, either connected or nonconnected, dispersed within it in either a regular or a random manner. The interconnected pores are termed effective pore spaces, and fluid can flow through a porous material only through the effective pore space. Muskat (1946) represented an ideal porous medium as a body of unconsolidated sand in which all the voids are interconnected so that the total pore space is equivalent to the effective pore space.

The flow of air through porous agricultural products has been an area of investigation for the past six decades beginning with Stirnimann et al. (1931). Questions raised by Wilhelm et al. (1981) and Segerlind (1983) suggest that significant further study is required. A knowledge of the air flow and pressure patterns in agricultural and biological products is necessary for determining cooling, heating, drying or aeration requirements. Numerical calculation of pressure and velocity flow fields associated with grain storage is difficult due to the uncertainty in the correct relationships and the tremendous variability in the material properties (Segerlind 1983). It is even more difficult with large round bales (both hard- and soft-core) of alfalfa material since the flow field is dependent on a number of parameters (porosity, pore size, etc.) that are difficult to quantify. Moreover, the actual process that occurs between the individual agricultural product and the flowing air is complex and not well understood (Talbot 1989). For this reason, the only feasible method of analysis is a macroscopic approach, one in which the values of variables under consideration are averages of indeterminate local values.

In the study of fluid flow through a porous medium a number of researchers have preferred correlating their experimental data heuristically because of the difficulty in accurately simulating the flow domain. Examples include Forchheimer (1901); Stirnimann et al. (1931); Henderson (1943); Shedd (1951, 1953); Ergun (1952); Osborne (1961); Bakker-Arkema et al. (1969); Gaffney and Baird (1977); Jayas and Muir (1991). Other researchers have employed numerical methods in simulating the flow domain (Marchant 1976a, 1976b; Nellist 1978; Rotz 1983; Talbot 1989).

There are basically two methods of data presentation (Eqs. 1 and 2) as recommended by Segerlind (1983), of these, Eq. 2 has consistently been demonstrated as being more representative of the experimental data.

$$\frac{dp}{dx} = av_s^n \tag{1}$$

$$\frac{dp}{dx} = av_s + bv_s^2 \tag{2}$$

where:

$dP/dX$ = pressure gradient through the media,

$v_s$ = velocity of the fluid, and

$a, b$ = constants representing material and fluid properties.

## MODEL DEVELOPMENT: POROUS MEDIUM APPROACH

A porous medium is characterized by a variety of geometric properties such as the porosity, specific internal surface area, tortuosity, etc. (Corey 1986). Soft-centre large round bales of forages may be considered complex porous media. Thus, fluid flow in such materials may be considered either as flow around submerged objects, flow in straight conduits in the packed column, or both. To develop a model that could be useful in predicting pressure gradient and velocity relationships in such a complex system requires that certain pertinent assumptions be made. Most porous media models have assumed characteristic particles in the bed to be spherical. The development in this study considered a piece of alfalfa stem as being cylindrical in shape and randomly dispersed throughout the bale.

### Model assumptions

The following assumptions were made in developing the equations governing airflow in large round bales.

1. The particles making up the bale are reasonably uniform in size and shape. End and wall effects are assumed negligible; that is, the number of particles adjacent to the entrance and the wall of the bale are few relative to the total number of particles in the bale. This assumption is valid when the diameter and depth of the bale are large in comparison with the diameter of individual particles.
2. The flow is steady-state and one directional.
3. The mean hydraulic radius of the flow paths is adequate to account for the variations in channel cross-sectional size and shape.
4. The total drag per unit area of channel wall is the sum of the viscous and inertial forces.
5. The equations developed are for the geometrically linear case (linear dimension, in X) and the effect of gravity is neglected.
6. Intercellular spaces within particles have an insignificant effect on the fluid flow and are, therefore, neglected. The pore spaces between particles are not sealed off and are reasonably uniform in size.
7. Fluid transport is in an isothermal and isotropic porous medium. The effect of anisotropy is assumed unimportant since flow is one-dimensional. Though the bale may be heterogeneous in general, it is assumed to be homogeneous perpendicular to the flow in the sections being analyzed. Any heterogeneity in the flow direction is accounted for by considering six distinct sections of the bale in the direction of flow.
8. The fluid is taken as incompressible.

## FLOW EQUATIONS

The basis for developing the equations governing incompressible airflow in the large round bales will be those presented by Bird et al. (1960). To reiterate, it is simply the sum of separately determined gradients due to viscous and turbulent forces. For laminar incompressible airflow through a circular tube, the pressure gradient is calculated as:

$$\frac{P_o - P_x}{X} = \frac{8\mu <V_i>}{R^2} \tag{3}$$

where:

$P_o$ = inlet static pressure,

$P_x$ = static pressure at a distance X,

$R$ = radius of tube,

$X$ = distance along tube length,

$<V_i>$= average velocity over a cross-sectional area, and

$\mu$ = fluid viscosity.

This is equivalent to Darcy's law in porous media flow.

The corresponding equation for turbulent flow through a circular tube, as presented by Bird et al. (1960), was:

$$\frac{P_o - P_x}{x} = \frac{1}{R}\frac{1}{4}\rho <V_i>^2 4f \tag{4}$$

where:

$\rho$ = fluid density, and

$f$ = Fanning friction factor.

In developing Eq. 4 for flow in a circular tube, Bird et al. (1960) noted that for highly turbulent flow in tubes with any appreciable roughness, the friction factor becomes a function of the roughness only. Considering the specifics of the porous media, several changes are made to the viscous and turbulent expressions to give them common independent variables. To allow the expressions originally developed for flow in tubes for that in bales, two changes are made to more accurately represent the conditions in bales. First, since there is no direct expression for the radius or diameter of the flow channels these terms are represented using a representative hydraulic radius, $R_m$. For the viscous expression, the radius, $R$, is exchanged for the hydraulic radius using $R = 2R_m$ (White 1986). Inserting this in Eqs. 3 and 4 results in:

$$\frac{P_o - P_x}{X} = \frac{2\mu <V_i>}{R_m^2} + \frac{1}{R_m}\frac{1}{2}\rho <V_i>^2 f_o \tag{5}$$

where:

$R_m$ = representative hydraulic radius, and
$f_o$ = equivalent friction factor in a packed bed .

Further substitutions are required to get the expression into a form which uses identifiable characteristics of the material making up the bale. First, the interstitial velocity, $V_i$, is expressed in terms of the apparent velocity, $V_s$, and the bale porosity, $\varepsilon$, using the Dupuit assumption (Bear 1972): $V_i = V_s/\varepsilon$. Recognizing the hydraulic radius as the ratio of the volume of fluid to the wetted surface area, $\omega$, it can be given as: $R_m = \varepsilon/\omega$. For a porous medium $\omega$ is given in terms of porosity and specific surface, $S$, as: $\omega = S(1-\varepsilon)$. Finally, using the definition given by Corey (1986), the specific surface is given as: $S = (2D_p + 4L)/D_pL$ for a cylinder of length $L$ and diameter $D_p$. Including all of these in Eq. 5 yields:

$$\frac{P_o - P_x}{X} = 2\mu\, V_s \frac{(2D_p + 4L)^2\,(1-\varepsilon)^2}{D_p^2 L^2 \varepsilon^3} + \frac{(2D_P + 4L)\,(1-\varepsilon)}{D_pL\varepsilon^3}\,\frac{1}{2}\rho V_s^2 f_o \tag{6}$$

where:

$D_p$ = cylinder diameter,
$L$ = cylinder length,
$V_s$ = apparent velocity,
$\varepsilon$ = bale porosity,
$\omega$ = wetted surface, and
$S$ = specific surface.

Equation 6 may further be simplified if one assumes that for an alfalfa stem the characteristic length, $L$, is much larger than the characteristic particle diameter, $D_p$ ($L >> D_p$). Hence, the aspect ratio $D_p/L$ may be assumed negligible ($D_p/L \approx 0$) leading to:

$$\frac{2D_p + 4L}{D_pL} = \frac{4}{D_p} \tag{7}$$

Inserting Eq. 7 into Eq. 6 yields;

$$\frac{P_o - P_x}{X} = \frac{32\mu\, v_s(1-\varepsilon)^2}{D_p^2\ \varepsilon^3} + \frac{2(1-\varepsilon)}{D_p\varepsilon^3}\rho\, V_s^2 f_o \tag{8}$$

The first term on the right side of Eqs. 6 and 8 represents the viscous components which are similar to Blake-Kozeny's (1927, cited in Bear, 1972) equations. The second term represents the inertial term and is similar to that presented by Burke and Plummer (1928). The parameters appearing in Eqs. 6 and 8 could be lumped into global coefficients, which may be used as indices for porous media in general and for large round bales in particular. In this study, $K_1$ and $K_2$ are chosen as the global coefficients for the viscous and inertial terms, respectively, as shown in Eq. 9 (similar to Forchheimer's empirical equation and one of those recommended by Segerlind, 1983):

$$\frac{P_o - P_x}{X} = K_1\, V_s + K_2\, V_s^2 \tag{9}$$

where $K_1$ and $K_2$ are global coefficients.

To obtain the values of $K_1$ and $K_2$ experimentally, it was necessary to measure pressure drops ($P_o$-$P_x$) across bales for various inlet or superficial velocities. Due to the variability of properties within these bales it was necessary to measure these at various sections in the direction of flow to not only determine values of $K_1$ and $K_2$ for a whole bale but also their variability throughout the bale. Because of the process in which large round bales are formed, the values of $K_1$ and $K_2$ change as one moves through the bale due primarily to changing porosity and, hence, bulk density.

## MATERIALS AND METHODS

Direct measurement of airflow characteristics was carried out in high moisture large round bales of alfalfa herbage. The apparatus (illustrated in Fig. 1) consisted of a fan/heater unit used to provide the required airflow. (The heater was not used in the present experiments.) The fan was connected to a duct equipped with a variable outlet orifice used to control the amount of airflow through the bale. Downstream of this, a bale was held in place by a sheet metal enclosure forcing essentially all the air through the bale. This was connected to the duct with an airtight canvas expansion section. For further details refer to Yiljep (1991).

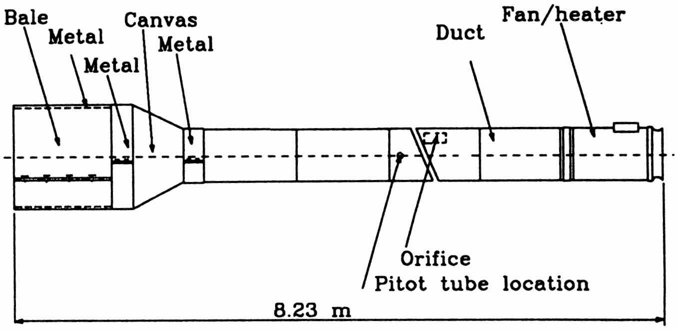

**Fig. 1. Schematic view of fan/heater experimental apparatus.**

### Bales

Using a soft-centre, variable chamber baler, large round soft-centre bales, 1.22 m long and 1.52 m in diameter, of alfalfa at various moisture contents (ranging from 46 to 60%, wet basis, depending on how long the herbage was wilted in the field) were formed in the summers of 1989 and 1990. Following baling, each bale was transported to the experimental site and characteristics such as mass were recorded. Initial masses of the bales were obtained using a commercial scale used for grain and other livestock feeds. Samples were taken at random from the fields for initial (pre-baling) moisture content determinations prior to forming the bales. Outside bale dimensions were essentially equal to that of the chamber giving a bale volume of 2.22 $m^3$.

### Airflow measurements

Each time a bale was mounted in the apparatus, airflow characteristics in terms of the entry static and velocity pressures in the duct extension (downstream of the orifice) were measured manually with a manometer which was connected to a pitot-static tube via a rubber tube 8 mm in diameter. Static pressures inside the bales were measured using the same manometer and rubber tube connected to a static pressure probe of about the same diameter as the rubber tube. The measurements were taken only axially since it was not possible to obtain measurements in both radial and axial directions due to the bale enclosure.

Velocity in the bale was determined by measuring the mean air velocity in the duct upstream of the bale and applying continuity to account for the larger bale area. Mean duct velocity was determined by measuring velocities at 14 locations across a section for each of four different settings of the orifice on the fan/heater outlet duct extension for each bale. Similarly, static pressure measurements were taken at cross-sections along the axis of the bale at distances of 0.00, 0.20, 0.41, 0.61, 0.81, 1.02, and 1.22 m into the bale. At each cross-section measurements were taken at 13 positions as shown in Fig. 2. Six readings per position were obtained for each of the 13 positions on the cross-section of a bale. Total head pressures were not measured inside the bales because of blockage of the velocity pressure probe orifices.

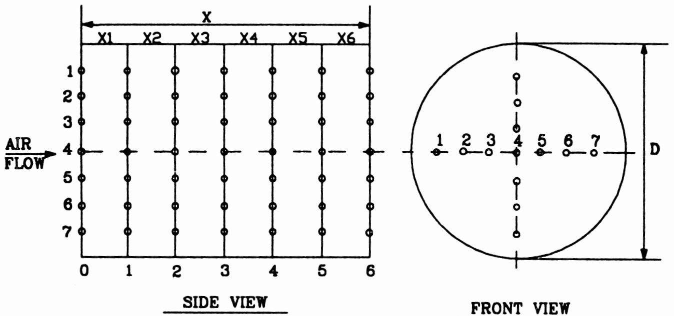

**Fig. 2. Schematic view of bale showing pressure sampling positions.**

## RESULTS AND DISCUSSIONS

### Physical properties of alfalfa material and large round bales

The pre-treatment characteristics in terms of days of field wilting ($DW$), size, initial average moisture content (wet basis) ($M_O$), initial mass ($W_O$), initial bulk density ($\rho_o$), and dry bulk density ($\rho_d$) of the alfalfa material and large round bales investigated are reported in Table I.

As seen in Table I, the longer the duration of field wilting of alfalfa material, the lower the average prebaling moisture contents (material wilted for the same days had similar average prebaling moisture contents). However, there was a considerable variation in the initial masses and bulk densities of the bales for given $M_O$ and $DW$ even though baled by the same baler. This variation may be attributed to variations in the topography of the field, windrow size within the field, herbage moisture content, speed of travel of the tractor and machine operation techniques.

### Static and velocity pressure measurement data

The variation in measured entry average static, $P_s$, and velocity, $P_v$, pressures as well as the apparent velocity appeared to depend on bale initial mass, initial bulk density, duration of field wilting of the material, and average prebaling (initial) moisture content. As depicted in Table II, the higher the initial masses and bulk densities of the bales (bales 1, 2, 4, and 5), the higher the values of the measured static pressures and the lower the velocity pressures for the various orifice area openings.

In general, duration of field-wilting and average prebaling moisture contents of the bales are poor predictors of the measured $P_s$ and $P_v$ variations across the fan/heater outlet duct extension. Alfalfa materials field-wilted for similar periods and showing similar average initial moisture contents indicated completely different $P_s$ and $P_v$ values. For example, the alfalfa material used in making bales 2 and 4 were both wilted for 2 days with average prebaling moisture contents of 48.2% and 47.5%, respectively (see Table I). Static pressure values were observed to be highest and velocity pressures lowest in bale 4 (compared to the rest of the bales studied in 1989); whereas, the opposite trends of $P_s$ and $P_v$ were observed in bale 2. This may be due to the mode of formation of the bales. Bale 4 also had the highest dry matter density, explaining its higher resistance to air flow.

In the 1990 experiments, similar trends of the dependence of measured static and velocity pressures on initial masses, bulk densities, duration of field-wilting and average prebaling moisture contents were observed. Bales 13, 14, and 18 with high initial masses and bulk densities resulted in higher $P_s$ and lower $P_v$ when tested. Placement of bales 15, 16, and 17 with low masses and bulk densities showed lower and higher entry $P_s$ and $P_v$, respectively, as observed in the 1989 studies. There was no evident influence of duration of field-wilting and prebaling moisture contents on $P_s$ and $P_v$.

Figures 3 and 4 show plots of average static pressures vs measurement positions across bale axial lengths for four average apparent velocities (corresponding to four orifice area openings). Note that a static pressure of 0.0 indicates atmospheric pressure. As seen in the plots, the average static

**Table I. Characteristics of alfalfa material and large round bales**

| Bale No.[a] | Duration of wilting (days) | Bale characteristics | | | |
|---|---|---|---|---|---|
| | | $M_o$ (%) | $W_o$ (kg) | $\rho_o$ (kg/m$^3$) | $\rho_d$ (kg/m$^3$) |
| 1 | 1.50 | 60.0 | 520 | 234 | 93.6 |
| 2 | 2.00 | 48.2 | 460 | 207 | 107.2 |
| 3 | 1.75 | 54.5 | 580 | 261 | 118.8 |
| 4 | 2.00 | 47.5 | 590 | 265 | 139.1 |
| 5 | 1.50 | 58.4 | 490 | 220 | 91.5 |
| 6 | 1.75 | 53.6 | 470 | 211 | 97.9 |
| 7 | 1.75 | 50.8 | 420 | 189 | 93.0 |
| 8 | 1.75 | 50.0 | 400 | 180 | 90.0 |
| 9 | 1.50 | 53.7 | 420 | 193 | 89.4 |
| 10 | 1.50 | 54.2 | 440 | 198 | 90.7 |
| 11 | 1.00 | 60.5 | 650 | 292 | 115.3 |
| 12 | 1.00 | 57.7 | 572 | 257 | 108.7 |
| 13 | 1.50 | 52.0 | 522 | 235 | 112.8 |
| 14 | 1.50 | 52.0 | 524 | 236 | 113.3 |
| 15 | 1.00 | 59.5 | 550 | 248 | 100.4 |
| 16 | 1.00 | 57.6 | 476 | 214 | 90.7 |
| 17 | 1.75 | 47.3 | 533 | 240 | 126.5 |
| 18 | 1.75 | 47.0 | 442 | 199 | 105.5 |

[a] Bales 1 to 12 are from 1989 experiments and 13 to 18 from 1990 experiments.

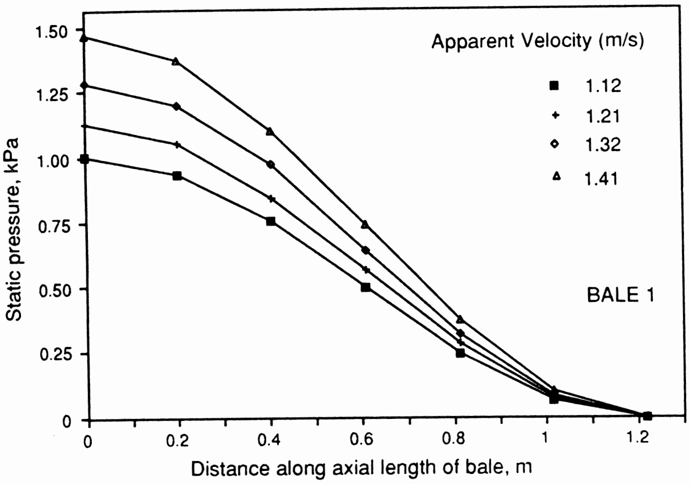

**Fig. 3. Static pressure vs axial length plots (Bale 1).**

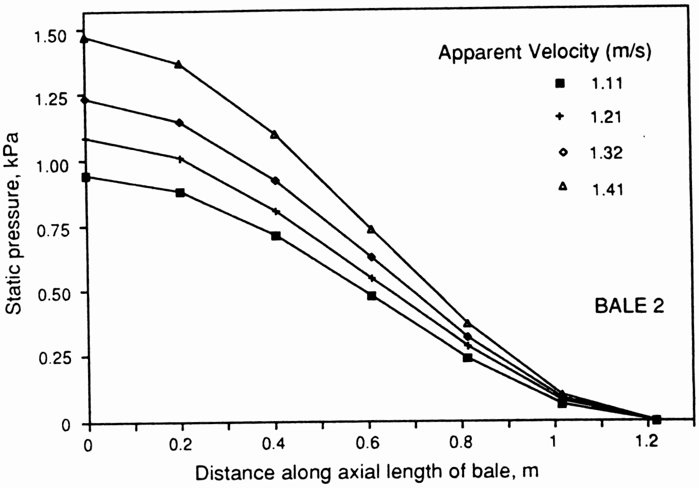

**Fig. 4. Static pressure vs axial length plots (Bale 2).**

pressure across bale axial lengths decreased with increasing distance from the inlet face. The slopes of the curves are highest in the centre and lowest in the outlet and inlet faces. This trend is similar in the plots for all the LRBs; however, there are distinct differences in the values and shapes of the curves. For bales studied in 1989 the higher the initial bale mass and bulk density, the higher the measured static pressures. This trend was not clearly defined for bales studied in 1990. The variation in static pressure between the bales may be due to the mode of formation and particle distribution within the LRBs. Average pressure gradients (pressure drop per unit length) from the static pressure data for the various distances across bale axial lengths and four orifice area openings (corresponding to four apparent velocities) were estimated. The various distances along the axial lengths of the bales were designated as sections $X_1$ to $X_6$ corresponding to distances 0.00 to 0.20 m, 0.20 to 0.41 m, 0.41 to 0.61 m, 0.61 to 0.81 m, 0.81 to 1.02 m, and 1.02 to 1.22 m from the inlet face, respectively.

Sample plots of the average pressure gradient-apparent velocity curves for bales 1 and 2 are shown in Figs. 5 and 6. It is seen that pressure gradients are highest at about the middle of each bale (sections $X_3$ and $X_4$), followed by sections $X_2$ and $X_5$ (near the centre) with the lowest gradients in all cases near the inlet and outlet faces of the bales ($X_1$ and $X_6$). This of course was also seen in the plots of Figs. 3 and 4. However, by presenting the data in this manner the striking similarities in measured average pressure gradients between any two opposite sections of a bale ($X_1$ vs $X_6$, $X_2$ vs $X_5$ and $X_3$ vs $X_4$) can also be seen. From this it is possible to deduce

## Table II. Entry average static/velocity pressures and apparent velocities at four orifice opening areas

| Bale No. | Orifice area ($m^2$) | Average duct pressure (Pa) | | Apparent velocity (m/s) |
|---|---|---|---|---|
| | | $P_s$ | $P_v$ | $V_{s2}$ |
| 1 | 0.046 | 1011 | 11.7 | 1.12 |
| | 0.031 | 1096 | 13,7 | 1.21 |
| | 0.015 | 1304 | 16.6 | 1.32 |
| | 0.000 | 1511 | 18.6 | 1.41 |
| 2 | 0.046 | 798 | 11.7 | 1.11 |
| | 0.031 | 903 | 13.7 | 1.21 |
| | 0.015 | 1028 | 16.6 | 1.32 |
| | 0.000 | 1147 | 18.6 | 1.41 |
| 3 | 0.046 | 793 | 9.8 | 1.00 |
| | 0.031 | 991 | 11.7 | 1.12 |
| | 0.015 | 1121 | 14.7 | 1.24 |
| | 0.000 | 1333 | 17.6 | 1.36 |
| 4 | 0.046 | 1123 | 0.9 | 0.98 |
| | 0.031 | 1239 | 11.7 | 1.11 |
| | 0.015 | 1448 | 13.7 | 1.20 |
| | 0.000 | 1634 | 16.6 | 1.32 |
| 5 | 0.046 | 934 | 11.7 | 1.10 |
| | 0.031 | 1046 | 13.7 | 1.20 |
| | 0.015 | 1171 | 16.6 | 1.32 |
| | 0.000 | 1358 | 19.6 | 1.42 |
| 6 | 0.046 | 838 | 11.7 | 1.12 |
| | 0.031 | 974 | 14.7 | 1.23 |
| | 0.015 | 1075 | 17.6 | 1.34 |
| | 0.000 | 1271 | 20.6 | 1.45 |
| 13 | 0.046 | 994 | 11.7 | 1.11 |
| | 0.031 | 1129 | 14.7 | 1.22 |
| | 0.015 | 1270 | 16.6 | 1.33 |
| | 0.000 | 1454 | 19.6 | 1.42 |
| 14 | 0.046 | 937 | 9.8 | 1.02 |
| | 0.031 | 1076 | 14.7 | 1.22 |
| | 0.015 | 1219 | 16.6 | 1.32 |
| | 0.000 | 1453 | 19.6 | 1.43 |
| 15 | 0.046 | 936 | 11.7 | 1.12 |
| | 0.031 | 1049 | 14.7 | 1.24 |
| | 0.015 | 1180 | 17.6 | 1.34 |
| | 0.000 | 1392 | 20.6 | 1.46 |
| 16 | 0.046 | 892 | 9.8 | 1.00 |
| | 0.031 | 1050 | 12.7 | 1.14 |
| | 0.015 | 1231 | 14.7 | 1.25 |
| | 0.000 | 1405 | 18.6 | 1.39 |
| 17 | 0.046 | 830 | 11.7 | 1.12 |
| | 0.031 | 940 | 14.7 | 1.24 |
| | 0.015 | 1105 | 17.6 | 1.34 |
| | 0.000 | 1216 | 19.6 | 1.44 |
| 18 | 0.046 | 1094 | 9.8 | 1.00 |
| | 0.031 | 1252 | 12.7 | 1.14 |
| | 0.015 | 1494 | 14.7 | 1.23 |
| | 0.000 | 1671 | 17.6 | 1.37 |

that in the axial direction, high-moisture, soft-centre large round bales of alfalfa herbage are symmetrical about a plane perpendicular to their axial centres. The variations in pressure gradients along the length of a bale, aside from measurement errors associated with the static pressure measurements, may be attributed to bulk porosity; hence, bulk density changes along the axial length of the bale. In general, the plots (Figs. 5 and 6) are close to straight lines, suggesting perhaps that only the viscous terms of Eq. 2 are important. However, fitting of the model with and without the inertial terms showed a noticeable improvement with the inertial terms present, indicating that both viscous and inertial terms are important in the resistance of soft-centre large round bales of alfalfa herbage to airflow.

### Parameter estimation

$K_1$ and $K_2$ in Eq. 14 for the various sections across bale axial lengths were estimated using the General Linear Modelling Procedure of the Statistical Analysis System (SAS 1988). Using the least squares method, unique values of $K_1$ and $K_2$ which best described the relationship between pressure gradient and apparent velocity for the various sections across bale lengths were determined. The estimated parameters, together with standard errors (SE) of model prediction of the experimental data are presented in Tables III and IV. As seen in the tables, the $K$ values are highest at about the middle of each bale and across all the LRBs (sections $X_3$ and $X_4$). This

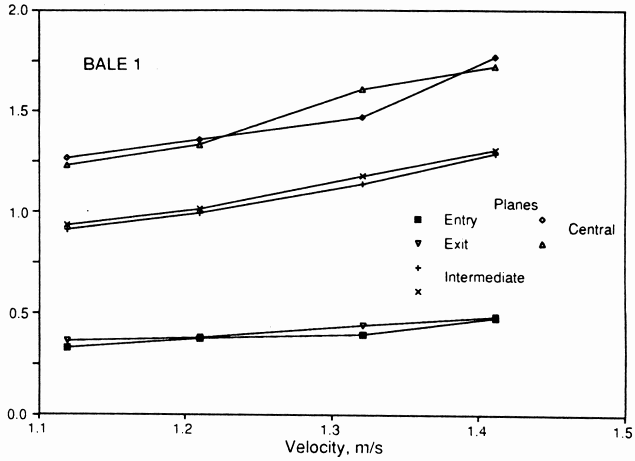

**Fig. 5. Pressure gradient vs velocity curves (Bale 1).**

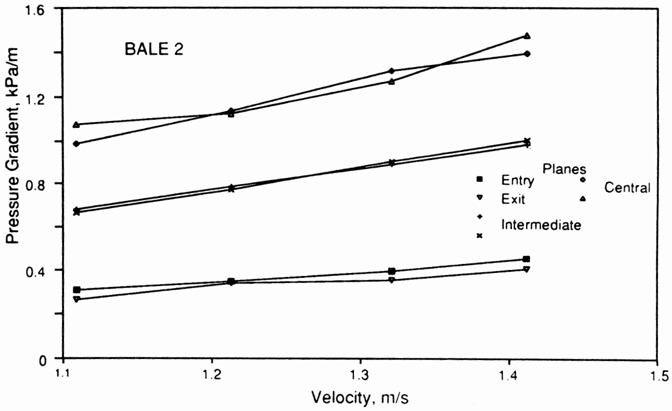

**Fig. 6. Pressure gradient vs velocity curves (Bale 2).**

**Table III. Estimated K values in planes across bale axial lengths**

| Bale No. | Paramenters | K* values Sections | | | | | |
|---|---|---|---|---|---|---|---|
| | | $X_1$ | $X_2$ | $X_3$ | $X_4$ | $X_5$ | $X_6$ |
| 1 | $K_1$ | 0.150 | 0.390 | 0.624 | 0.503 | 0.422 | 0.226 |
| | $K_2$ | 0.132 | 0.368 | 0.421 | 0.522 | 0.358 | 0.084 |
| 2 | $K_1$ | 0.110 | 0.301 | 0.531 | 0.608 | 0.167 | 0.101 |
| | $K_2$ | 0.148 | 0.283 | 0.334 | 0.291 | 0.388 | 0.132 |
| 3 | $K_1$ | 0.082 | 0.407 | 0.565 | 0.644 | 0.361 | 0.068 |
| | $K_2$ | 0.202 | 0.329 | 0.451 | 0.413 | 0.363 | 0.221 |
| 4 | $K_1$ | 0.124 | 0.668 | 0.943 | 0.914 | 0.624 | 0.162 |
| | $K_2$ | 0.303 | 0.285 | 0.420 | 0.487 | 0.304 | 0.266 |
| 5 | $K_1$ | 0.110 | 0.315 | 0.582 | 0.624 | 0.370 | 0.127 |
| | $K_2$ | 0.164 | 0.392 | 0.407 | 0.367 | 0.348 | 0.150 |
| 6 | $K_1$ | 0.085 | 0.257 | 0.448 | 0.465 | 0.270 | 0.070 |
| | $K_2$ | 0.156 | 0.387 | 0.394 | 0.384 | 0.380 | 0.173 |
| 13 | $K_1$ | 0.095 | 0.278 | 0.511 | 0.658 | 0.263 | 0.175 |
| | $K_2$ | 0.173 | 0.459 | 0.527 | 0.416 | 0.467 | 0.114 |
| 14 | $K_1$ | 0.232 | 0.614 | 0.743 | 0.720 | 0.536 | 0.167 |
| | $K_2$ | 0.075 | 0.203 | 0.321 | 0.331 | 0.251 | 0.130 |
| 15 | $K_1$ | 0.096 | 0.338 | 0.447 | 0.527 | 0.399 | 0.150 |
| | $K_2$ | 0.172 | 0.355 | 0.493 | 0.430 | 0.306 | 0.127 |
| 16 | $K_1$ | 0.062 | 0.512 | 0.748 | 0.814 | 0.540 | 0.070 |
| | $K_2$ | 0.242 | 0.264 | 0.371 | 0.316 | 0.235 | 0.235 |
| 17 | $K_1$ | 0.084 | 0.312 | 0.463 | 0.446 | 0.308 | 0.058 |
| | $K_2$ | 0.166 | 0.271 | 0.434 | 0.447 | 0.276 | 0.183 |
| 18 | $K_1$ | 0.100 | 0.739 | 0.887 | 1.069 | 0.553 | 0.565 |
| | $K_2$ | 0.206 | 0.450 | 0.282 | 0.338 | 0.376 | 0.327 |

* Units of $K_1$ are (kPa - s/m$^2$), and $K_2$ are (kPa - s$^2$/m$^3$).

**Table IV. Standard errors of model prediction of pressure gradients in sections across length of bales**

| Bale No. | Standard errors of estimate Sections | | | | | |
|---|---|---|---|---|---|---|
| | $X_1$ | $X_2$ | $X_3$ | $X_4$ | $X_5$ | $X_6$ |
| 1 | 1.68 | 1.74 | 6.59 | 3.63 | 1.45 | 0.91 |
| 2 | 0.65 | 0.26 | 2.41 | 4.41 | 0.53 | 1.65 |
| 3 | 0.23 | 1.22 | 4.56 | 5.38 | 2.46 | 1.39 |
| 4 | 0.99 | 1.61 | 6.30 | 3.98 | 1.16 | 0.84 |
| 5 | 0.96 | 4.00 | 3.36 | 2.97 | 2.17 | 1.12 |
| 6 | 0.14 | 2.71 | 3.55 | 3.97 | 0.59 | 0.97 |
| 13 | 1.75 | 2.01 | 3.22 | 4.17 | 4.36 | 0.80 |
| 14 | 0.50 | 4.27 | 9.17 | 9.56 | 5.10 | 1.31 |
| 15 | 1.39 | 3.90 | 4.93 | 4.61 | 2.48 | 0.71 |
| 16 | 1.54 | 5.69 | 3.81 | 2.20 | 5.89 | 1.05 |
| 17 | 0.60 | 0.15 | 3.30 | 5.15 | 1.88 | 1.67 |
| 18 | 2.63 | 2.94 | 5.15 | 8.08 | 3.40 | 1.80 |

may be attributed to uneven distribution of the alfalfa herbage resulting in denser middle sections of the LRBs during their formation. Another possible explanation could be that since most biological materials including alfalfa are viscoelastic, lateral expansion and probable redistribution of the particles on the outlet and inlet faces of the bales after ejection from the baler may account for more uniform flow characteristics and hence, more accurate predictions at the faces. However, this phenomenon was not investigated further in this study.

In general, the model (Eq. 9) followed the data in sections across bale axial lengths reasonably well. Based upon the relative magnitudes of $K_1$ and $K_2$, viscous forces were more pronounced in planes $X_2$ to $X_5$ while inertial forces dominated in planes nearer the inlet and outlet sections of the bales. The coefficients of determination ($R^2$) were consis-

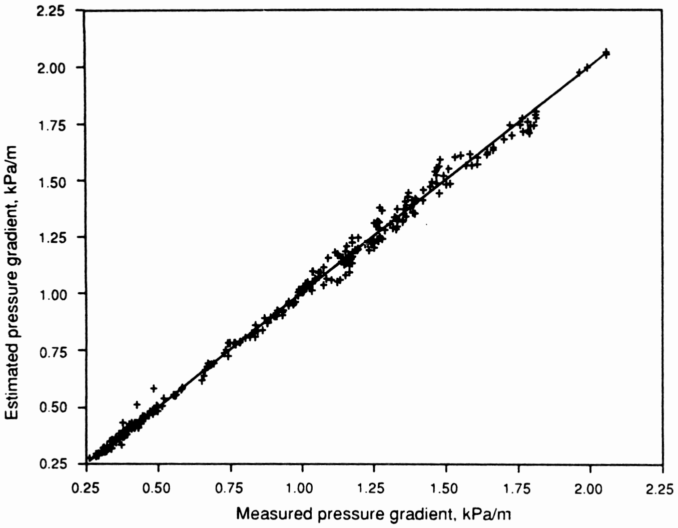

**Fig. 7. Combined plot of estimated vs observed pressure gradients (for both 1989 and 1990 bales).**

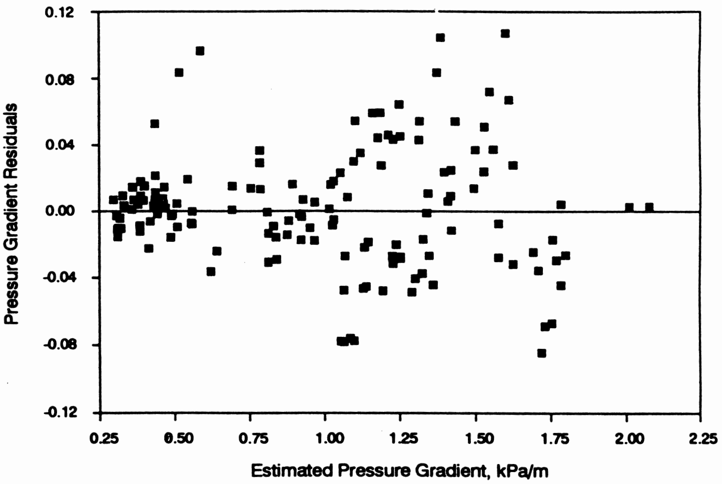

**Fig. 8. Combined plot of residuals vs estimated pressure gradients (for both 1989 and 1990 bales).**

tently high, never falling below 0.92 for any of the cases considered. Values of $K$ reported in the literature ranged from $K_1 = 0.00895$ to 16.6 s/m and $K_2 = 0.005$ to 7.96 $s^2/m^2$ for sand (Fancher and Lewis 1933). In his study on particulate transport through a porous medium (coarse sand), Joy (1989) reported $K$ values ranging from $K_1 = 3.5$ to 70 s/m and $K_2$ = 120 to 40,000 $s^2/m^2$. Such values for high-moisture large round bales of alfalfa herbage have not been reported previously in the literature. When the results are expressed in similar units (84.9 multiplied by those in Table IV) they range from $K_1 = 4.93$ to 90.8 s/m and $K_2 = 6.37$ to 44.8 $s^2/m^2$. These are within the range of the values reported previously for materials ranging from fine sands to coarse gravels. Differences between the general model (Eq. 6) and its reduced form (Eq. 8) will be reflected in porosity synthesis across the bales and will be reported in another paper.

### Model assessment

The model was further assessed by plotting the predicted pressure gradients against the measured pressure gradients (combined for both 1989 and 1990 bales) as shown in Fig. 7. The line of perfect fit is also shown. While some scatter is expected, it is seen that in general, the model follows the data reasonably well over the range of soft-centre large round bales of alfalfa tested. The residuals were plotted against predicted pressure gradients as shown in Fig. 8. Random scatter of the residuals are observed as would normally be expected for a good fit.

## SUMMARY AND CONCLUSIONS

A general one-dimensional mathematical model was developed based on the concept of fluid flow in porous media for the purpose of predicting pressure gradient-apparent velocity relationships in large round bales. The general model was further simplified by assuming that particle aspect ratio was negligible. Global viscous and inertial coefficients were estimated using least squares regression analysis for sections across the bale axial lengths. Based on the results of this study the following conclusions can be drawn:

1. There was no evident influence of duration of field-wilting and prebaling moisture contents on measured static and velocity (dynamic) pressures. This is probably due to such factors as windrow size, speed of tractor travel, topography of the field and to machine operation techniques which led to much wider variations than those due to duration of field-wilting and moisture content.
2. The slopes of pressure gradient-apparent velocity curves are highest in the axial centres and lowest around the inlet and outlet sections of the bales. This indicates proportionately higher losses in the centre sections due to higher density as a result of inherent machine operation.
3. Similar slopes in these same curves at the entry and exit sections suggests that soft-centre large round bales are symmetrical about a plane perpendicular to their axial centres.
4. Graphs of pressure gradient vs velocity do not plot as straight lines, indicating that both viscous and inertial terms are important in the resistance of the bales to airflow.
5. Estimated global viscous and inertial coefficients in the bales were within the range for porous media reported in the literature for granular materials.

## ACKNOWLEDGEMENT

The authors acknowledge the financial support of the Ontario Ministry of Agriculture and Food for this research.

## REFERENCES

Anon. 1989. Canadians see sales improvement in 1989. *Implement and Tractor* 104(1):9.

Bakker-Arkama, F.W., R.J. Patterson and W. Bickert. 1969. Static pressure-airflow relationships in packed beds of granular biological materials such as cherry pits. *Transactions of the ASAE* (12):134-136.

Bear, J. 1972. *Dynamics of Fluids in Porous Media*. New York, NY: American Elsevier.

Bird, R.B., W.E. Stewart and E.N. Lightfoot. 1960. *Transport Phenomena*. New, York, NY: John Wiley and Sons Inc.

Burke, S.P. and W.P. Plummer. 1928. Gas flow through packed columns. *Industrial and Engineering Chemistry* 20:1197-1200.

Collins, R.E. 1961. *Flow of Fluids through Porous Materials*. New York, NY: Reinhold Publishing Corp.

Corey, A.T. 1986. *Mechanics of Immiscible Fluids in Porous Media*. Littleton, CO: Water Resources Publications.

Ergun, S. 1952. Fluid flow through packed columns. *Chemical Engineering Progress Series* 48(2):89-94.

Fancher, G.H. and J.A. Lewis. 1933. Flow of simple fluids through porous materials. *Industrial and Engineering Chemistry* 25:1139-1147.

Forchheimer, D. 1901. Wassebewegung durch boden. *Zeitschrift Das Verines Deutsch Ing*. 49:1736-1749.

Gaffney, J.J. and C.D. Baird. 1977. Forced air cooling of bell peppers in bulk. *Transactions of the ASAE* 20(6):1174-1179.

Henderson, S.M. 1943. Resistance of shelled corn and bin walls to air flow. *Agricultural Engineering* 24(11):367-369.

Jayas, D.S. and W.E. Muir. 1991. Airflow-pressure drop data for modelling fluid flow in anisotropic bulks. *Transactions of the ASAE* 34(1):251-254.

Jayas, D.S., S. Sokhansanj, E.B. Moysey and E.M. Barber. 1987. Airflow resistance of canola (rapeseed). *Transactions of the ASAE* 30(5):1484-1488.

Joy, D. 1989. Particulate transport in porous medium. Unpublished Ph.D. thesis, University of Waterloo, Waterloo, ON.

Marchant, J.A. 1976a. The prediction of fan pressure requirements in the drying of large hay bales. *Journal of Agricultural Engineering Research* 21:333-346.

Marchant, J.A. 1976b. The prediction of airflow in crop drying systems by finite element method. *Journal of Agricultural Engineering Research* 21:417-429.

Muskat, M. 1946. *The Flow of Homogeneous Fluids through Porous Media*. Ann Arbor, MI: J.W. Edwards Inc.

Nellist, M.E. 1978. Crop drying and mathematical models. NCAE-NIAE Operational Workshop, Silsoe, U.K.

Osborne, L.E. 1961. Resistance to airflow of grain and other seeds. *Journal of Agricultural Engineering Research* 6(2):119-122.

Plue, P.S. and W.K. Bilanski. 1991. Airflow and temperature patterns through large round bales. *Applied Engineering in Agriculture* 7(5):525-529.

Rotz, A.C. 1983. Economics of chemically conditioned alfalfa on Michigan dairy farms. ASAE Paper No. 83-1640. St. Joseph, MI: ASAE.

SAS. 1988. SAS User's Guide: Statistics. Release 6.03. SAS Institute Inc., Box 8000, Cary, NC.

Segerlind, L.J. 1983. Presenting velocity-pressure gradient data for use in mathematical models. *Transactions of the ASAE* 26(4):1245-1248.

Shedd, C.K. 1951. Some new data on resistance of grains to air flow. *Agricultural Engineering* 32(9):493-496.

Shedd, C.K. 1953. Resistance of grains and seeds to air flow. *Agricultural Engineering* 34(9):616-619.

Stirnimann, E.J., G.P. Bodnar and E.N. Bates. 1931. Tests on resistance to the passage of air through rough rice in a deep bin. *Agricultural Engineering* 12(5):145-148.

Talbot, M.T. 1989. Pressure patterns established by commercial element package. ASAE Paper No. 89-6039. St. Joseph, MI: ASAE.

White, F.M. 1986. *Fluid Mechanics*, 2nd ed. New York, NY: McGraw-Hill.

Wilhelm, L.R., F.D. Tompkins and C.A. Mullins. 1981. Airflow resistance of lima beans and southern peas. ASAE Paper No. 81-3034. St. Joseph, MI: ASAE.

Yiljep, Y.D. 1991. Airflow resistance and the effects on nitrogen solubility of heat-processing large round bales of alfalfa herbage. Unpublished Ph.D. thesis, University of Guelph, Guelph, ON.